Received: 5 July 2018 | Revised: 6 September 2019 | Accepted: 10 October 2019 | Published on: 15 November 2019

DOI: 10.1002/joc.6362

RESEARCH ARTICLE

International Journal of Climatology RMetS

# Past and future impact of the winter North Atlantic Oscillation in the Caspian Sea catchment area

**Sri D. Nandini-Weiss**[1] | **Matthias Prange**[1] | **Klaus Arpe**[2] | **Ute Merkel**[1] | **Michael Schulz**[1]

[1]MARUM – Center for Marine Environmental Sciences and Faculty of Geosciences, University of Bremen, Bremen, Germany

[2]Max-Planck-Institute for Meteorology, Hamburg, Germany

**Correspondence**
Sri D. Nandini-Weiss, Institute of Oceanography, Center for Earth System Research and Sustainability (CEN), University of Hamburg, Hamburg, Germany.
Email: sri.durgesh.nandini-weiss@uni-hamburg.de

**Funding information**
H2020 Marie Skłodowska-Curie Actions, Grant/Award Number: 642973

## Abstract

The Caspian Sea level (CSL) has undergone variations of more than 3 m during the past century with important implications for the life of coastal people, economy and the ecosystem. The origin of these variations as well as future changes in the Caspian water budget are still a matter of debate. Here, the major modes of North Atlantic winter climate variability and atmospheric teleconnections that have a potential effect on the hydroclimate of the Caspian catchment region are examined. The skill of the Community Earth System Model (CESM1.2.2) regarding the simulation of the modern climatology in the Caspian region and the major North Atlantic modes are analysed using different atmospheric grid resolutions and setups of the atmospheric component, the Community Atmosphere Model (CAM4 and CAM5). CESM1.2.2 with CAM5 atmosphere physics and 1° atmospheric grid resolution shows reasonable skill in simulating the regional Caspian basin climatology and the winter North Atlantic Oscillation (NAO). Using this model version, a weakly positive ($r = .2$) statistically significant ($p < .05$) correlation between the catchment winter water budget (precipitation minus evaporation, P-E, integrated over the catchment area) and the NAO is found for the historical period 1850–2000. Climate projections of the 21st century under the Representative Concentration Pathways RCP4.5 and RCP8.5 show that the NAO remains the leading mode of winter variability with a dominant influence on the climate in the Caspian catchment region. Under the RCP4.5 scenario the correlation between the winter NAO and winter P-E over the Caspian catchment region increases ($r = .5$, $p < .05$). For RCP8.5, however, this correlation disappears due to a north–south dipole pattern with a positive P-E anomaly over the northern and a negative anomaly over the southern parts of the Caspian catchment region, cancelling out an effect on the total Caspian water budget. Nevertheless, due to increasing annual evaporation over the Caspian Sea in the warming climate, the model predicts an additional CSL decrease of about 9 and 18 m between

2020 and 2100 for the RCP4.5 and RCP8.5 scenarios, respectively. Even though the model tends to overestimate the total evaporation due to a too large Caspian Sea surface area, these values are larger than previous projections of CSL decline.

**KEYWORDS**

Caspian Sea level, CESM1.2.2, North Atlantic Oscillation (NAO), precipitation minus evaporation (P-E), RCP4.5, RCP8.5

## 1 | INTRODUCTION

The Caspian Sea (CS) is the world's largest inland sea and located within a closed (endorheic) drainage basin (Figure 1). The CS is nestled between eastern Europe and central Asian semi-arid regions, northern flat terrains and Caucasus high mountain ranges. The CS catchment basin (covering ca. $3.7 \times 10^6$ km$^2$) is ca. 10 times larger than the CS itself, and includes more than 130 rivers feeding into the lake (Rodionov, 1994; Arpe *et al*., 2019). The Volga River is the main inlet (~80–90% of total river discharge into the CS) and covers the northern CS catchment basin (Leroy *et al*., 2019). The other major river basins include Ural, Terek, and Kura. The CS basin is rich in ecosystems, large river systems, and major wetlands and features high level species endemism and diversity (Kosarev, 2005). Therefore, climatic changes in this region may have a strong environmental impact.

The CS has experienced drastic lake level changes due to climate and hydrological processes in the last 150 years (Arpe *et al*., 1999; Arpe and Leroy, 2007; Kroonenberg *et al*., 2008; Chen *et al*., 2017). Currently, the Caspian Sea level (CSL) is ~28 m below zero (i.e., the global sea level). However, during the past 150 years, large and rapid fluctuations of ~4 m in CSL (−25 to −29 m) had strong consequences for coastal communities. The drivers for these changes are not fully understood and heavily debated (Golitsyn *et al*., 1990; Rodionov, 1994; Arpe *et al*., 2000; Elguindi and Giorgi, 2006b; Arpe and Leroy, 2007; Kislov *et al*., 2014; Panin *et al*., 2014; Panin and Dianskii, 2014). However, numerous observational and modelling studies suggest that variations in the CSL are mainly driven by climate-induced changes in the Volga river runoff and surface fluxes (precipitation minus evaporation, P-E) over the CS (Elguindi and Giorgi, 2007; Kroonenberg *et al*., 2008; Panin *et al*., 2014; Yanina, 2014; Panin *et al*., 2015; Chen *et al*., 2017). Due to the CSL's sensitivity to hydroclimatic changes, future risk assessment and the development of adaptive strategies are of particular importance in the CS region.

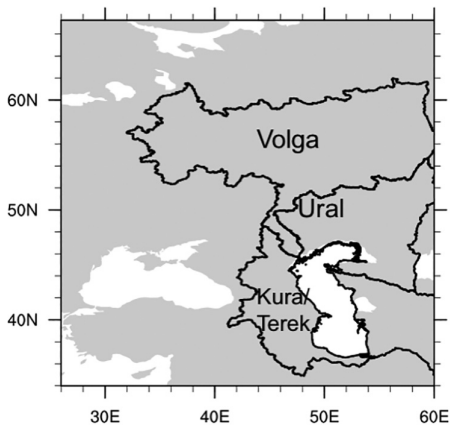


**FIGURE 1** Caspian catchment area and major river basins outlined in black

Atmospheric circulation features influencing the CS catchment area include the mid-latitude westerly winds and, at upper tropospheric levels, the polar and subtropical jet streams (Rodionov, 1994; Molavi-Arabshahi *et al*., 2015). Several air masses affect the regional climate, that is, cold air from the Arctic, moist temperate air masses from the Atlantic Ocean, warm subtropical air masses arising from the Black Sea, and dry continental air masses from the east. Hence, the northern CS resides in a continental climate zone, whereas the central and southern CS is located in a warm and dry climate belt. Given this complex climatological setting, the seasonal cycle of precipitation varies strongly over the different regions of the catchment area, with maximum precipitation in summer over the northern part (Volga basin), in spring over the western part (Kura/Terek area), and in autumn-winter over the southern CS (the eastern CS coastal area is a desert). Evaporation over the CS is highest in autumn (September) (Rodionov, 1994).

Major winter North Atlantic teleconnection patterns are known to impact European climate and include the North Atlantic Oscillation (NAO), the East Atlantic (EA) pattern and the Scandinavia (SCA) pattern (Barnston and Livezey, 1987; Hurrell, 1995; Panin and Dianskii, 2014). Although the NAO, EA, and SCA patterns undoubtedly have a strong impact on European winter climate, their influence on the hydrology of the Caspian catchment region and hence the CSL is controversial. While Rodionov (1994) discusses possible effects of the NAO on the CSL and Panin and Dianskii (2014) as well as Panin *et al*. (2015) argue in favour of NAO-driven CSL changes based on correlations between NAO and precipitation, other studies

could not find a stable connection between NAO and CSL, but instead suggest a role of the El Niño-Southern Oscillation (ENSO) in driving CSL variations (Arpe *et al*., 2000). Recent studies have evaluated the ability of climate models to reproduce teleconnection patterns and revealed biases in representing physical processes and shifts in the position and magnitude of the centres of action that impact regional surface temperature and precipitation (Stoner *et al*., 2009; Lee and Black, 2013; Davini and Cagnazzo, 2014; Ning and Bradley, 2016). These studies emphasize the need to consider teleconnection biases in projections of future climate change and their relationships with regional winter climate variability.

Moreover, projections for the 21st century CSL change remain contradictory since much depends on the model physics and resolutions and the key underlying assumptions that lead to different results (Elguindi and Giorgi, 2006a; Elguindi and Giorgi, 2006b; Arpe and Leroy, 2007; Renssen *et al*., 2007). CSL predictions were performed based on global (Arpe *et al*., 1999; Kislov and Toropov, 2007; Renssen *et al*., 2007; Kislov *et al*., 2014) and regional models (Elguindi and Giorgi, 2006b, 2007). Using a global model and projections based on the IPCC A1B scenario, Renssen *et al*. (2007) show a CSL decline of 4.5 m by 2100. Projections based on the IPCC A2 scenario suggested a CSL decline of at least five meters by 2100 (Elguindi and Giorgi, 2007). Interestingly, by using an ensemble of different atmosphere–ocean general circulation models (AOGCMs) forced by the same A2 scenario, a CSL drop of about nine meters by the end of 2100 was found (Elguindi and Giorgi, 2006a). Other models suggested a stable or even increasing CSL (Arpe and Leroy, 2007). Hence, it is essential to consider biases from model setups and resolutions to improve our understanding regarding the physical mechanisms behind future CSL variations.

In the present study, we investigate the potential role of North Atlantic winter teleconnections in driving regional Caspian climate variability and CSL variations with the coupled general circulation model CESM1.2.2. Given the potential sensitivity of simulated teleconnections and hydroclimatic variations to model physics and grid resolution as mentioned above, we carry out a model evaluation to select the best model version with respect to atmosphere physics and horizontal resolution to represent the CS catchment climate. We also investigate the changing influence of the winter NAO on the Caspian region hydroclimate under global warming for the period 1850–2100. Moreover, we provide first-order estimates of the projected CSL change under two emission scenarios by the end of the 21st century.

## 2 | METHODOLOGY AND DATA

### 2.1 | Model and experimental design

The Community Earth System Model CESM1.2.2 is a fully coupled global climate model (Hurrell *et al*., 2013). Its development is coordinated by the National Center for Atmospheric Research (NCAR), Boulder, Colorado. The coupled components include a physics based atmospheric model (Community Atmosphere Model, CAM4 or CAM5), a land-surface model (Community Land Model, CLM4.0) (Lawrence *et al*., 2011), an ocean general circulation model (Parallel Ocean Program, POP2) (Smith *et al*., 2010), a dynamic-thermodynamic sea ice model (Community Ice CodE, CICE4) (Hunke and Lipscomb, 2010) and a River Transport Model (RTM at 0.5° resolution) (Gent *et al*., 2011). The models are coupled through the CESM1.2.2 flux coupler (CPL7). The CESM1.2.2 ocean and ice models share the same horizontal grid. The horizontal resolution of this grid varies and is higher around Greenland, with the North Pole displaced, as well as around the equator. In all our experiments, we use a nominal 1° resolution of the ocean/sea–ice grid. The ocean model grid has 60 levels in the vertical.

CESM1.2.2 can be run with different atmospheric grid resolutions and physics packages (CAM4 and CAM5). CAM5 differs from CAM4 by simulating full aerosol-cloud interactions and hence indirect radiative effects. It includes improved moist turbulence, shallow convection, cloud micro- and macrophysics, and aerosol schemes (see Neale *et al*., 2012 for details). CAM4 runs with 26 levels in the vertical, while four levels were added for a better representation of the boundary layer in CAM5. To evaluate which model version performs best with regard to CS basin climatology and North Atlantic modes of variability, we carried out three control transient experiments (Table 1) using different atmospheric grid resolutions (2° versus 1°) and model physics (CAM4 versus CAM5) for the historical (1850–2005 AD) period with identical forcings (a combination of anthropogenic and natural forcings; see Gent *et al*. (2011); Meehl *et al*. (2012)) and on the same machine (Cray XC30/40 of HLRN-III). Note that the atmosphere model has a finite volume dynamical core with a uniform horizontal resolution which is shared with the land model grid.

In order to examine potential future changes in the climate of the CS region, two transient experiments were run until the year 2,100 under the IPCC scenarios RCP4.5 and RCP8.5 (Moss *et al*., 2010; Meinshausen *et al*., 2011; van Vuuren *et al*., 2011). The RCP8.5 is a high-range scenario with rising greenhouse gas emissions and a radiative forcing

**TABLE 1** CESM1.2.2 coupled model experiments

| Experiment | Resolution: Horizontal grid | Period |
|---|---|---|
| Control CAM4 | 2° (2.5 × 1.9°) | 1850–2005 CE |
| Control CAM4 | 1° (1.25 × 0.9°) | 1850–2005 CE |
| Control CAM5 | 1° (1.25 × 0.9°) | 1850–2005 CE |
| RCP4.5 CAM5 | 1° (1.25 × 0.9°) | 2005–2100 CE |
| RCP8.5 CAM5 | 1° (1.25 × 0.9°) | 2005–2100 CE |

of 8.5 W/m$^2$ by the year 2,100 while RCP4.5 is a mid-range scenario that does not exceed 4.5 W/m$^2$ (Lamarque *et al*., 2011). Both experiments use the 1° version of CAM5 and were initialized with the final state of the corresponding historical run. Experiments are summarized in Table 1.

## 2.2 | Observational/reanalysis climate data

The following datasets were used to assess the model's skill in simulating the climate of the Caspian region and North Atlantic teleconnection patterns. Sea-level pressure (SLP) from 1950–2000 at 2.5° resolution was taken from the National Center for Environmental Prediction (NCEP/NCAR) reanalysis dataset (Kalnay *et al*., 1996). Gridded (at 0.5° resolution) monthly station time series of land 2-m temperature (T2 m) is taken from the University of Delaware dataset version 4.0.1 (Willmott and Matsuura, 1995) for the period 1900–2000. Mean monthly precipitation, evaporation and P-E reanalysis data at 0.5° resolution was extracted from the reanalysis done at the European Center for Medium Range Weather Forecasts (ECMWF) (Dee *et al*., 2011) for the period 1979–2000. For the analysis of the total hydrological budget of the Caspian catchment basin, we integrated P-E over the entire basin area up to 60° E where the Karakum Desert (Turkmenistan) is located and river water from further east evaporates and seeps away (Figure 1).

## 2.3 | Climate indices

We apply Empirical Orthogonal Function (EOF) analysis to the observational, reanalysis and model data to extract independent modes of climate variability in the North Atlantic/European region. The NAO, EA and SCA indices in this study are defined as standardized first, second and third principal component time series calculated from seasonal-mean SLP anomalies in the region [70°W–60°E, 20°–80°N], which includes the CS basin. We focus on the winter season, Dec-Jan-Feb (DJF), as the NAO and other modes display their largest climate impact in the boreal winter months (Arpe *et al*., 2000; Arpe et al., 2014; Hurrell et al., 2003; Hurrell *et al*., 2013). All data was detrended before performing the EOF analysis. Corresponding maps (spatial patterns) were obtained by regressing the detrended SLP fields onto the standardized principle component time series (index). The time series of each mode was obtained by projecting the eigenvectors of the SLP covariance matrix onto the latitude-weighted anomalies (North *et al*., 1982). The signs of the NAO, EA and SCA indices are defined such that a positive NAO phase corresponds to a negative SLP anomaly over Iceland (Hurrell, 1995), a positive EA phase corresponds to a positive SLP anomaly over the Northeast Atlantic (Barnston and Livezey, 1987) and a positive SCA phase is related to a positive SLP anomaly over Scandinavia (Bueh and Nakamura, 2007; Aondover, 2013).

# 3 | RESULTS

## 3.1 | Simulation skills of CESM1.2.2 for the modern climatology of the Caspian Sea region and North Atlantic modes of variability

We evaluate the skills of the different model setups in simulating climatological 2-m air temperature (T2 m), precipitation and evaporation (defined here as the total surface moisture flux into the atmosphere) fields in the CS catchment [36–60°N; 45–55°E] by means of a Taylor diagram (Figure 2), which is a common practice to evaluate multiple aspects of a climate model's performance in a single diagram (Taylor, 2001). To this end, the three historical runs with different model setups (Table 1) are evaluated against observational/reanalysis datasets for climatological (1979–1999) annual means. The Taylor diagram reveals that all model setups show lowest skill (low spatial correlation) for evaporation, whereas the models perform better with respect to T2 m and precipitation. One reason for the relatively low skill in simulating the evaporation field is related to the land-sea mask of CESM1.2.2, where the CSL is set to global sea level and therefore the CS surface area is too large especially in the north (Figure S1, S2). Since evaporation mainly takes place over the CS, this results in a positive bias in all the model simulations (Figure 2). As a consequence, the water budget of the Caspian catchment basin becomes too negative (Figure S3, S4). A negative bias in the simulation of precipitation (Figure 2) further contributes to the negative water

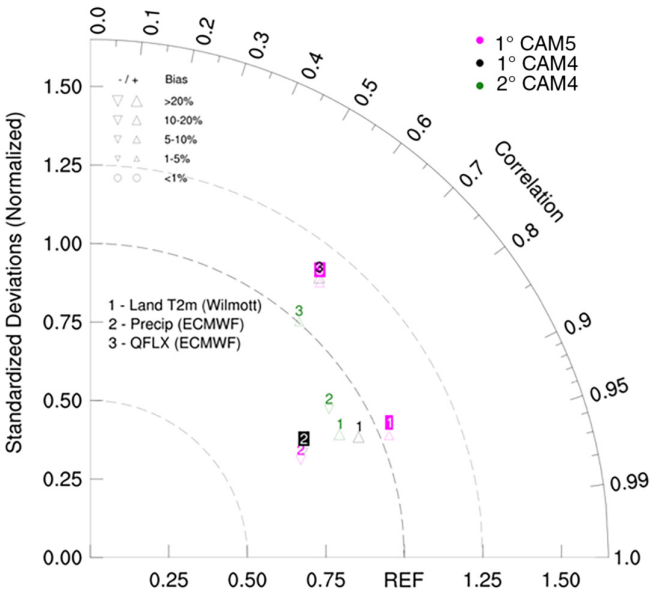


**FIGURE 2** Normalized Taylor diagram for different CESM versions and the referenced data variables (annual means) over the Caspian basin [36–60°N, 45–55°E] (1979–1999). The QFLX here refers to evaporation. The diagram shows CESM-data correlation coefficients (angular axis), CESM standard deviations normalized to observational standard deviations (radius) and biases (Baker and Taylor, 2016; Taylor, 2001)

budget in all model setups and is partly related to a poor simulation of precipitation in the mountainous regions (Caucasus, Elburz) to the west and south of the CS (Figure S5, S6). This orography-related bias is smallest in the 1° model setups. With respect to T2 m the 1° CAM5 setup shows the smallest bias over the entire region (Figure 2). A closer inspection reveals that a temperature bias north of the CS of more than 4°C in the 2° CAM4 setup reduces to less than 2°C in the 1° CAM5 setup (Figure S7, S8).

Figure 3 shows the first, second, and third modes of North Atlantic SLP winter variability as simulated by the three model setups and derived from reanalysis data for the period 1950–1999. The results reveal that the simulation with 1° CAM5 shows the best skill when compared to the first mode derived from reanalysis data with respect to the spatial EOF patterns and explained variances, that is, 46.4% in the model compared to 42.7% in the reanalysis data. All model setups have severe problems with simulating an EA-like pattern (second mode) and a SCA-like pattern in the third mode, but the 2° CAM4 setup clearly shows the poorest performance compared to the reanalysis. The NAO pattern (seen from the first mode) is also simulated by both

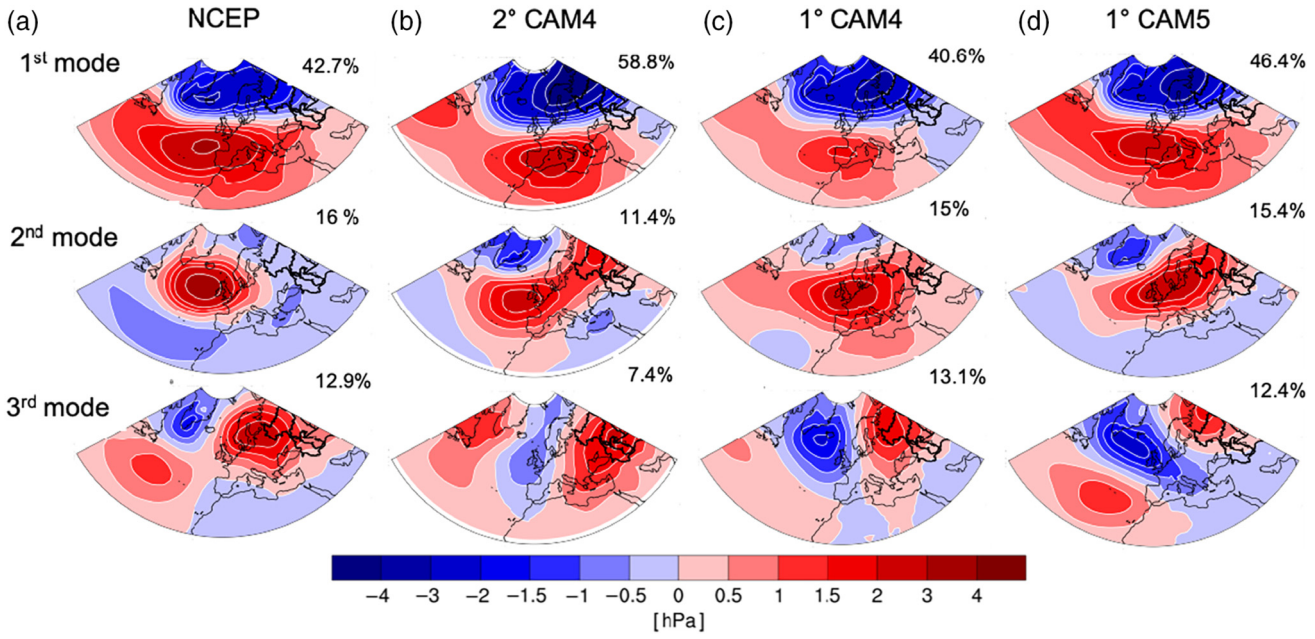


**FIGURE 3** Leading modes of winter (DJF) SLP (detrended) variability calculated for 1950–1999 [70°W–60°E, 20°–80°N] from (a) reanalysis data and (b–d) different model versions. Maps were obtained by regressing the detrended SLP fields onto the standardized principal components. The black outline denotes the Caspian catchment basin

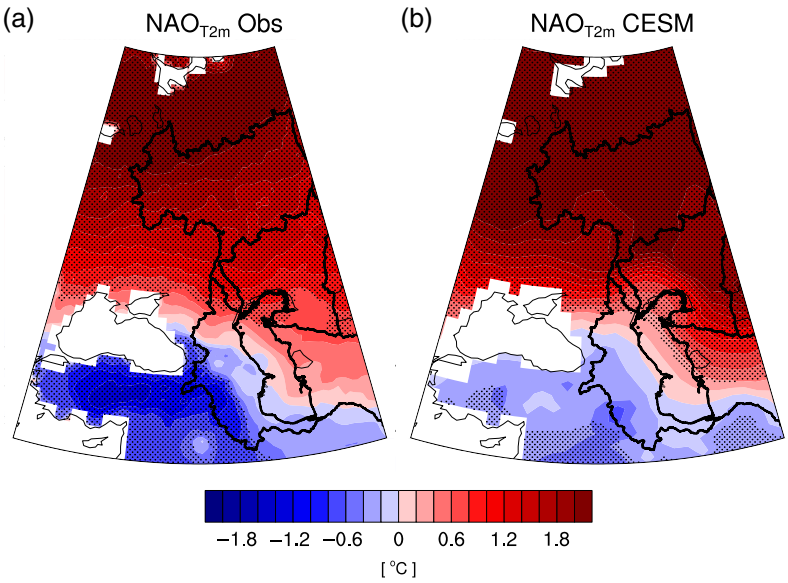


**FIGURE 4** Detrended winter (DJF) near-surface temperature (T2 m) regressed onto the leading standardized principal component of DJF SLP (NAO index, cf. Figure 3) from (a) observations/reanalysis and (b) CESM (1° CAM5) for 1950–1999. Stippling indicates significance at 95% level (applying Student's *t*-test). The black outline denotes the Caspian catchment basin

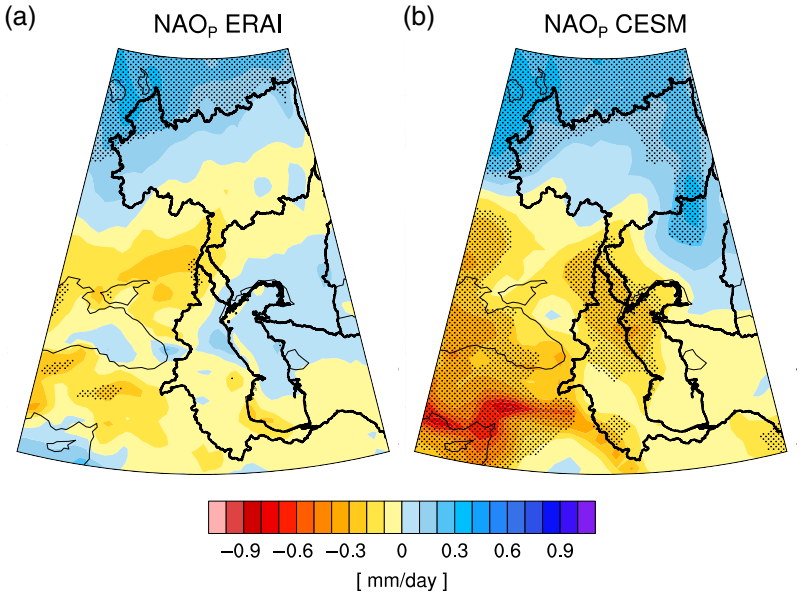


**FIGURE 5** As Figure 4 but for detrended DJF precipitation and the period 1979–1999

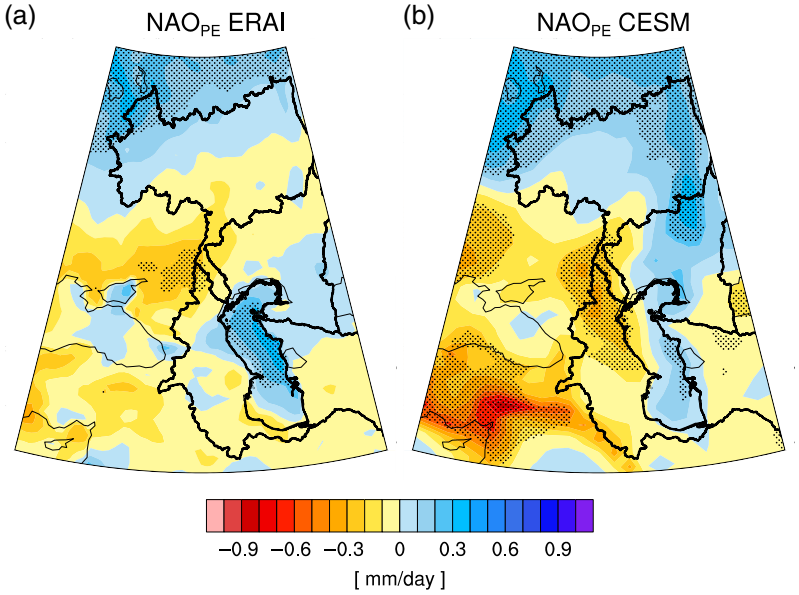


**FIGURE 6** Same as Figure 5, but for P-E

CAM4 model setups, but the NAO southern centre of action is too weak in the 1° CAM4 while the northern centre of action is shifted eastward in all model setups. Taken together, the 1° CAM5 setup shows considerably improved skill in simulating the leading modes of variability compared to the 1° CAM4 and 2° CAM4 setups. It is important to identify the difference between the model setups for future climate change studies. Based on our evaluation, we carried out CESM simulations for future climate with the 1° CAM5 setup. Moreover, we restrict our further analyses to the first mode (NAO), since the simulations of the second and third modes (EA and SCA) are still insufficient with this model setup. Since the position and intensity of teleconnection centres of action are known to affect regional temperature and precipitation, the model biases need to be considered in the assessment of past and future changes in the Caspian region (Hurrell, 1995; Stoner *et al*., 2009; Ning and Bradley, 2016).

## 3.2 | Influence of NAO on winter temperature, precipitation and P-E in the Caspian catchment area

In order to analyse the influence of the NAO on the winter (DJF) climate in the Caspian catchment region, we calculate linear regression coefficients with the detrended T2 m, precipitation and P-E fields. The regressions are tested for significance against the null hypothesis (i.e., slope = 0). Figure 4 shows the results for observations and the 1° CAM5 version of CESM1.2.2 for temperature and the period 1950–1999. The model captures the observed pattern related to the NAO rather well (Figure 4a, b). In both model and observations, the nodal line crosses the CS and, further to the west, the Black Sea. During the positive NAO phase anomalous warming occurs over the northern part of the Caspian catchment region (including the Volga river basin), while anomalous cooling takes

place in the southwestern part. The anomalous warming is mainly controlled by advection of heat by anomalous westerly flow as shown in previous studies (Hurrell and van Loon, 1997; Trigo *et al*., 2002) and linked to the anomalous SLP pattern over the larger CS area (cf. Figure 3a, d).

As to precipitation, both data and model show a strong and large-scale negative anomaly west of the Caspian catchment region (Mediterranean/Black Sea region) and a positive anomaly over the northern Volga basin during the positive NAO phase (Figure 5). It has been shown that NAO-related changes in the mean flow are accompanied by a meridional shift in the storm tracks and associated synoptic eddy activity (Hurrell and van Loon, 1997), which in turn controls precipitation rates (Trigo *et al*., 2002), thus explaining wetter/drier conditions in the northern/southern regions during positive NAO (Figure 5). P-E shows a strong NAO signal over the CS in the reanalysis with a positive anomaly during the positive NAO phase (Figure 6a). A positive anomaly is also simulated by the model, albeit weaker compared to reanalysis over the CS and stronger over the Volga basin (Figure 6b).

The explained variance for the historical period (1850–2000) as simulated by the 1° CAM5 version is 44.9% for the NAO which exhibits a north-eastward shift of the northern centre of action with respect to reanalysis data (Figure 7). A trend analysis of the corresponding principal component time series showed no significant trend over the historical period. Considering the impact of the NAO over the entire historical period (1850–2000) in order to obtain more reliable statistics, we find that the T2 m pattern remains robust (Figure 8a) when compared to the shorter period (Figure 4b). The winter EOF-based NAO index for this period is significantly correlated with the winter T2 m averaged over the catchment area ($r = .7$, $p < .05$). The winter precipitation shows a much more pronounced and significant large-scale north–south dipole over the longer period than over the shorter late 20th century interval, with more impact on the Caspian catchment area (Figure 8b). This precipitation pattern reflects a northward shift in the storm track and increased moisture transport which is associated with a shift in winter precipitation from southern to northern Europe and the Volga catchment (Hurrell, 1995; Hurrell and van Loon, 1997). This results in a slightly positive correlation between the winter NAO index and winter precipitation averaged over the CS catchment area ($r = 0.2$, $p < .05$). The P-E pattern largely resembles the precipitation pattern (Figure 8c). Anomalous Volga basin precipitation dominates the relationship between NAO and the catchment-integrated water balance, resulting in a weak but statistically significant positive correlation between

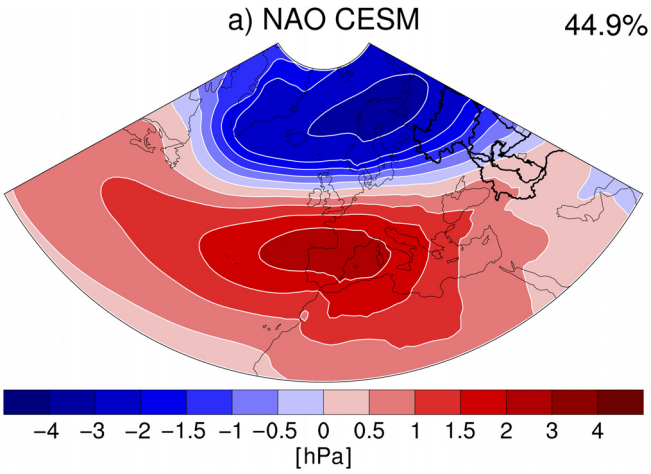


**FIGURE 7** Leading mode as in Figure 3 but for the historical period 1850–2000 using CESM with 1° CAM5

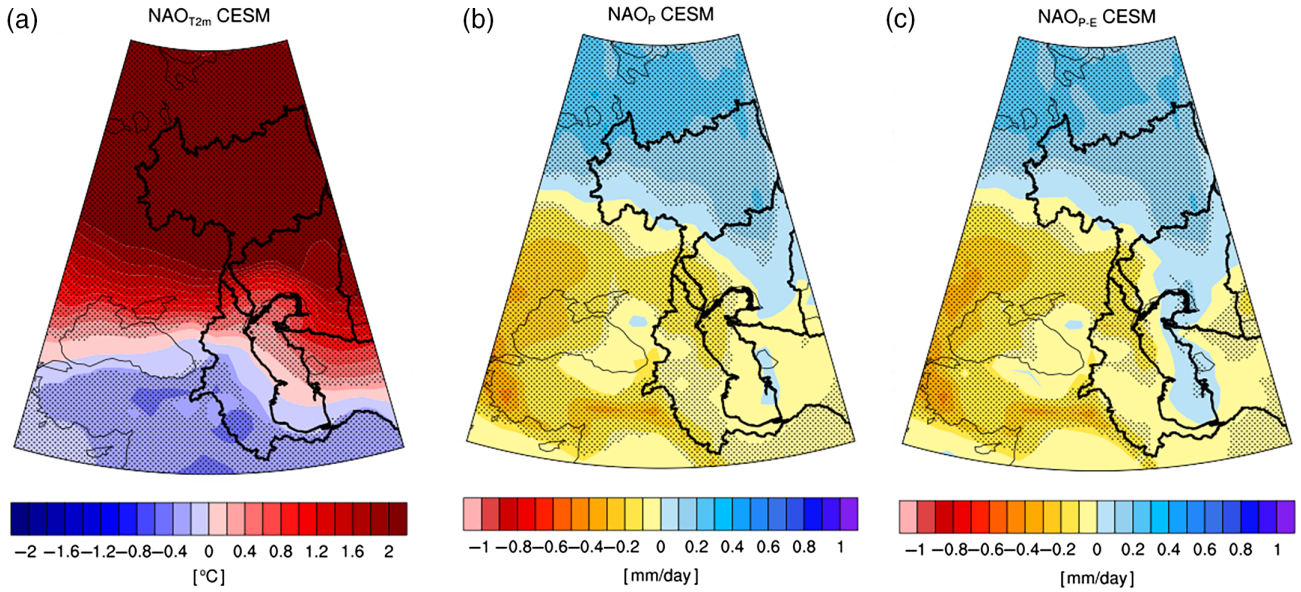


**FIGURE 8** As Figures 4–6 but for the simulated historical period 1850–2000 with CESM with 1° CAM5

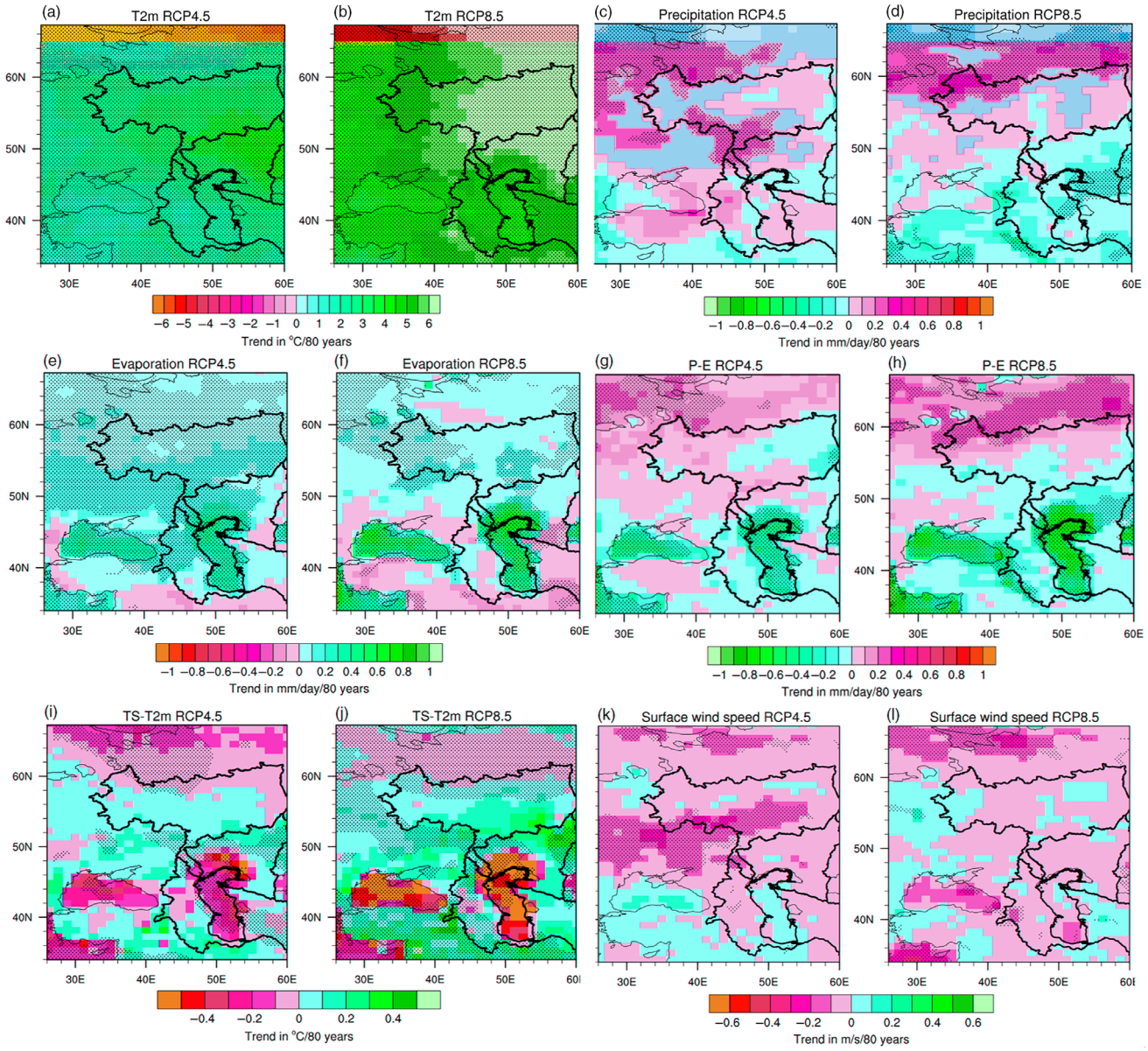


**FIGURE 9** Linear trends of annual mean in the RCP4.5 and RCP8.5 scenarios with CESM 1° CAM5 for the period 2020–2100 for (a, b) T2 m, (c, d) precipitation, (e, f) evaporation, (g, h) P-E, (i, j) surface temperature minus 2 m air temperature (TS-T2 m) and (k-l) surface windspeed. Stippling indicates significance at the 95% level (applying Student's *t*-test)

the winter NAO index and winter P-E integrated over the Caspian catchment area ($r = 0.2$, $p < .05$).

## 3.3 | Projected climatic changes in the Caspian catchment area

Here we examine the projected mean climatological changes first and then investigate the projected changes in the winter NAO signal and its influence on winter Caspian hydroclimate. Regarding projections of the future CS climate evolution, we only consider the 21st century long-term trends based on annual means (2020–2100), since on shorter (e.g., decadal) timescales the transient behaviour of future climate change is influenced by internal climate variability, for example, the NAO (Deser *et al.*, 2017). Consideration of the long-term trend minimizes the effects of internal climate variability in our analysis. Figure 9 shows the linear trends (slopes) in annual mean T2 m and hydroclimatic variables as simulated with the 1° CAM5 setup of CESM1.2.2 for the RCP4.5 and RCP8.5 scenarios. In the RCP4.5 scenario the warming is weaker but the pattern has a similar structure (Figure 9a). As expected, the RCP8.5 simulation shows a strong annual warming over the entire region, which is slightly dampened over the water bodies (Caspian Sea, Black Sea) (Figure 9b).

The RCP4.5 shows precipitation increases over the northern and western CS basin, whereas a north–south dipole structure

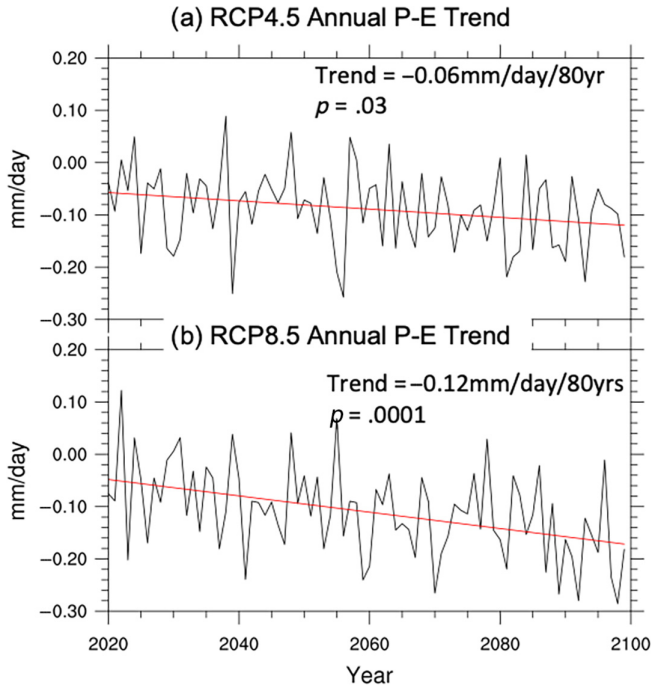


**FIGURE 10** Trend analysis of P-E timeseries based on annual means integrated over the CS catchment area over 80 years (2020–2100) for (a) RCP4.5 and (b) RCP8.5 as simulated by CESM (1° CAM5)

emerges in the RCP8.5 scenario (Figure 9c,d). Evaporation also increases in response to the warming. Strong increase of evaporation over the CS contributes to the damping of surface warming over the lake area. The increase in evaporation dominates over the precipitation increase such that P-E decreases over the Caspian catchment area in both scenarios (Figure 9e–h). The increase in evaporation over the CS in the RCP8.5 scenario amounts to 15–20% by the end of the 21st century, which is in line with the 16% global lake evaporation increase recently found by Wang *et al*. (2018) under the same emission scenario. Due to evaporative cooling and thermal inertia of water the lake surface warms slower than the air above in both warming scenarios but especially more so for the RCP8.5 (Figure 9i,j) which implies a higher stability of the atmospheric boundary layer and therefore attenuates increased evaporation. No significant changes in surface wind speed are found over the CS that would contribute to enhanced lake evaporation in the global warming scenarios (Figure 9k, l).

The timeseries of future annual mean P-E integrated over the CS catchment area shows significantly ($p < .05$) decreasing trends (−0.06 mm/day/80 years for RCP4.5 and − 0.12 mm/day/80 years for RCP8.5) (Figure 10). Based on a simple "bathtub" model of the CS, which ignores the bathymetry of the CS as in Elguindi and Giorgi (2006a), and taking a value of 10 for the ratio between CS catchment area and CS surface area, the above negative P-E trends translate into an additional reduction of the CSL by ca. 9 m (RCP4.5) and 18 m (RCP8.5) from 2020 to 2100. Table 2 shows the projected P-E trends (2020–2100) based on seasonal means integrated over the CS catchment for RCP4.5 and RCP8.5. The future P-E is negative for all seasons except the winter, highlighting the dominance of future enhanced evaporation, especially for the summer under the RCP4.5 and the autumn for the RCP8.5. In both scenarios, only in winter a positive trend is found, which can be attributed to an increase in precipitation over the Volga basin (Figure 11) that was also noted in previous studies (Elguindi and Giorgi, 2007). We note that the annual catchment-integrated P-E had no significant long-term trend for the historical period. Increasing evaporation due to warming becomes dominant only in the 21st century, whereas no significant warming of the CS was simulated for the historical period (not shown). By analysing the historical period, Arpe and Leroy (2007) suggested that it is the summer precipitation over the Volga which is key to past CSL variations. However, our linear trend analysis for P-E anomalies suggests that it is the increase in summer (under RCP4.5) and spring and autumn (RCP8.5) evaporation over the CS catchment area that is key to understanding future CSL changes by 2100.

**TABLE 2** Linear trend analysis (in mm/day/80 years) with significance ($p$-values; bold for $p < .05$) for P-E time series (2020–2100) integrated over the CS catchment for RCP4.5 and RCP8.5 and the individual seasons

| Seasons | RCP4.5 P-E | RCP8.5 P-E |
|---|---|---|
| DJF | Trend = 0.1 ($p = .1$) | Trend = 0.11 ($p = .08$) |
| MAM | Trend = −0.02 ($p = .6$) | Trend = **−0.16** ($p =$ **.02**) |
| JJA | Trend = **−0.18** ($p =$ **.003**) | Trend = **−0.11** ($p =$ **.02**) |
| SON | Trend = −0.13 ($p = .07$) | Trend = **−0.33** ($p =$ **.0001**) |

Note: The bold values are statistically significant.

## 3.4 | Projected changes in the NAO signal and influence on winter Caspian Hydroclimate

Of particular interest in this study is the projected winter NAO influence on the CS catchment area. Under RCP4.5 and RCP8.5 we find that NAO remains the leading mode of North Atlantic winter variability but the location and intensity in the centres of action slightly change (Figure 12). No significant trend is found in the projected NAO index in our simulations. The projected NAO pattern is hard to be distinguished from the present-day NAO pattern given the present-day model biases (Figures 3, 7). Under RCP4.5, the only clear difference is that the NAO's northern centre of action is more intensified, extended to the east and has a stronger impact on the entire CS catchment area, while the southern centre of action is weaker, resulting in a southward shift of the nodal line (Figure 7 versus Figure 12a). Compared to the RCP4.5, in the RCP8.5 scenario the model predicts a more (less) intensified southern (northern) centre of

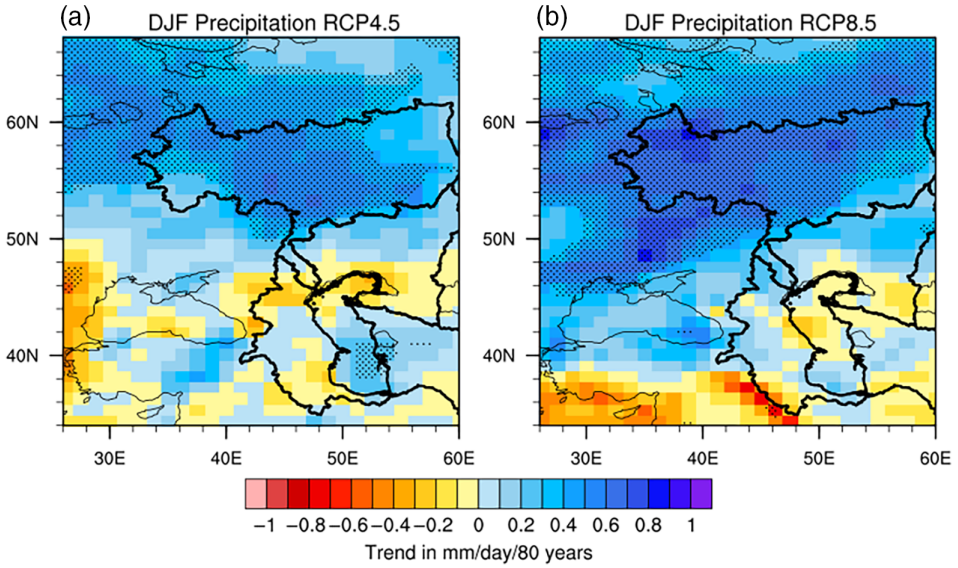


**FIGURE 11** As Figure 9c,d but for winter (DJF) seasonal means

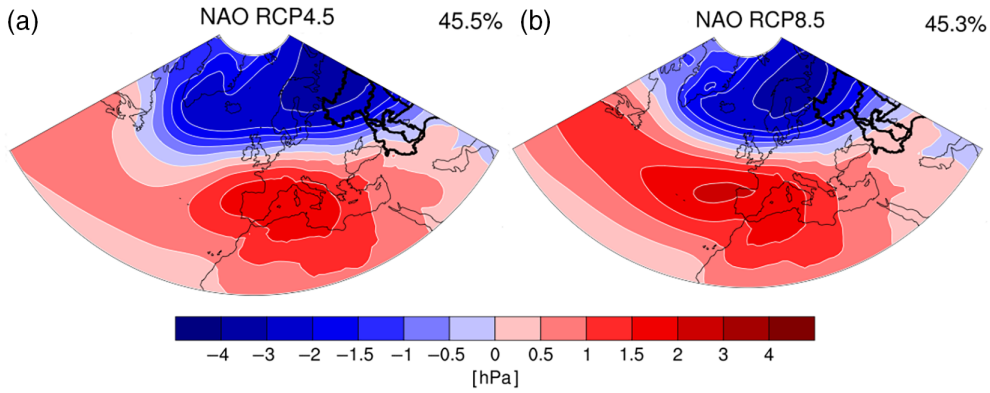


**FIGURE 12** Same as in Figure 7 but for 2020–2100 in (a) RCP4.5 and (b) RCP8.5

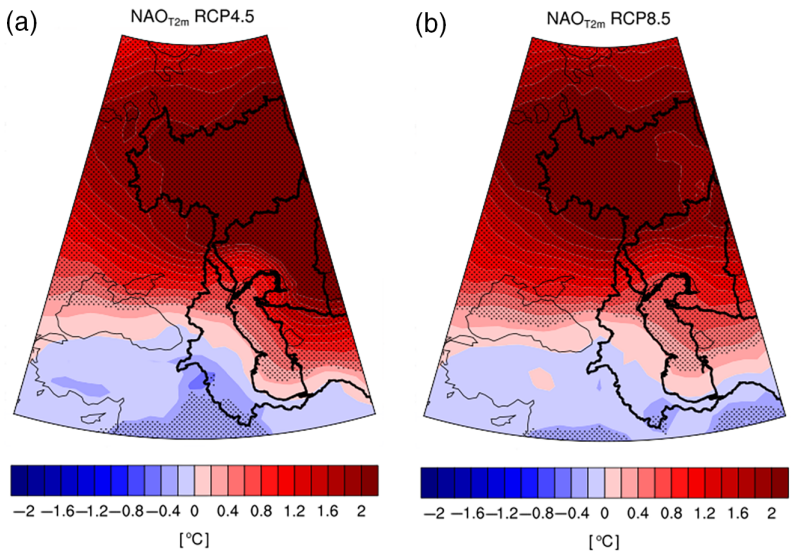


**FIGURE 13** As Figure 8a but for 2020–2100 in (a) RCP4.5 and (b) RCP8.5

action, with a smaller southward displacement of the nodal line over the CS region (Figure 12b). These projected shifts in the nodal lines are likely related to future changes in the large-scale SLP pattern with SLP decrease over the Arctic and increase over the Atlantic and southern European regions (Collins *et al*., 2013).

Regressing the detrended winter T2 m onto the winter NAO index for the period 2020–2100 we find a clear north–

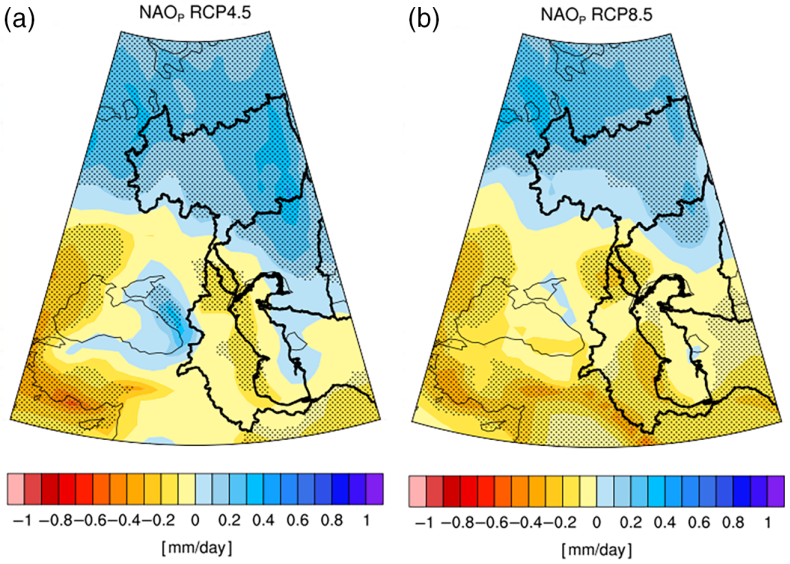


**FIGURE 14** Same as Figure 13 but for precipitation

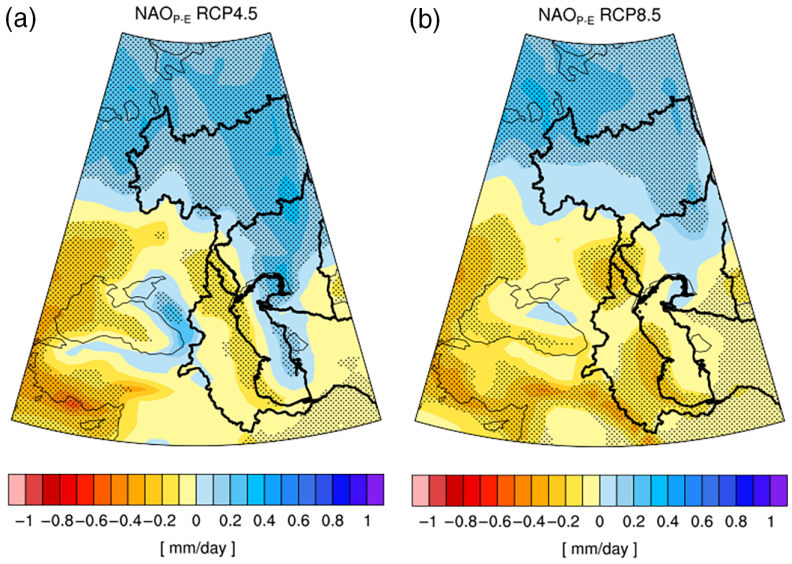


**FIGURE 15** Same as Figure 13 but for P-E

south dipole pattern for both RCP4.5 (more southward displaced) and RCP8.5 (less southward displaced over the CS compared to RCP4.5) (Figure 13). Hence, compared to the present/historical situation (Figure 8), the region of positive temperature anomalies during the positive NAO phase extends further south in both scenarios such that almost the entire Caspian basin and Black Sea experience a surface air temperature increase during the positive NAO phase.

In both scenarios, T2 m for almost the entire Caspian catchment is in phase with NAO since the nodal line shifts southward compared to present. The particularly strong correlation between NAO and CS catchment-averaged T2 m under RCP4.5 ($r = .73$, $p < .05$) compared to RCP8.5 ($r = 0.63$, $p < .05$) is likely driven by the shift and intensification of the northern center of action.

Compared to the present situation, the influence of NAO on winter precipitation is projected to increase in the northern part of the Caspian catchment area in RCP4.5 (with a correlation of $r = .5$ for the catchment average, $p < .05$) (Figure 14a). However, in RCP8.5 NAO's influence on winter precipitation increases over the southern part of the catchment region (Figure 14b) which can partly be attributed to a northward shift of the EOF's nodal line and an intensified southern center of action in SLP (Figure 12b). This can be linked to a poleward shift in the storm tracks which is accompanied by a poleward shift in midlatitude precipitation (Yin, 2005; Meehl *et al*., 2007; Chang *et al*., 2012). Moreover, a change in the frequency and magnitude of winter blocking events during NAO may also affect precipitation over the southwestern CS (Molavi-Arabshahi *et al*., 2015).

As to P-E, a distinct north–south dipole pattern emerges in RCP8.5 (Figure 15) which gives rise to a net cancellation of the effect of winter NAO on P-E variability integrated over the entire Caspian catchment area (i.e., the Caspian

water budget) as a positive (negative) P-E anomaly over the Volga basin is nearly compensated by a negative (positive) P-E anomaly over the southern basins. Under the RCP4.5 scenario the correlation between the winter NAO index and winter P-E integrated over the Caspian catchment area (detrended) increases significantly ($r = 0.5$, $p < .05$). For RCP8.5, however, this correlation disappears ($r = .05$, $p = .6$) and the prominent P-E dipole pattern removes the net NAO effect on the Caspian water budget due to a sub-basin cancellation which is linked to the mechanisms of the NAO-precipitation relationship discussed above. However, in both scenarios the future long-term evolution of catchment-integrated P-E and hence CSL will not be determined by changes in the NAO, but rather by gradually increasing evaporation that will lead to a substantial CSL decline over the 21st century.

## 4 | DISCUSSION

The 1° CAM5 setup of CESM1.2.2 simulates the leading mode of North Atlantic winter variability (NAO) with reasonable skill. The CESM teleconnection for the Caspian region is reliable for the NAO, and reproduces typical see-saw spatial patterns in temperature and precipitation which just reach the CS catchment area. The DJF NAO has a clear influence on the DJF T2 m as also seen in other studies (Hurrell and Deser, 2009; Comas-Bru and McDermott, 2014; Deser *et al*., 2017). Due to the large meridional extension (ca. 30° latitude) and complex orography of the CS catchment area, the NAO affects different parts of the catchment in different ways. A positive NAO reflects enhanced and northward shifted westerly flow bringing warm (and moist) maritime air as far east as the CS region. Associated variations in the precipitation pattern are linked to anomalous atmospheric moisture transport and synoptic activity driven by the NAO as shown previously (Trigo *et al*., 2002; Panin *et al*., 2015). While previous studies hypothesized an effect of the NAO on the total Caspian water budget (integrated P-E) and hence CSL (Panin and Dianskii, 2014; Panin *et al*., 2015), we were able to quantify this correlation for the historical period based on CESM1.2.2 ($r = .2$, $p < .05$).

Our results suggest that the relationship between the NAO and the catchment-integrated winter P-E changes depends on the respective background winter climate and the chosen timescale. Under RCP4.5, the projected changes in NAO-driven winter temperature and precipitation signals in the CS region are attributed to an intensified and northeasterly displaced northern center of action along with a weakened southern center of action when compared to the present-day situation, while in the RCP8.5 scenario NAO-related changes are attributed to a comparably more intense and westward shifted southern center of action. Even though there is no general consensus on shifts in the NAO centers of action under changing climate conditions, a similar northeastward shift in the NAO is also seen for some models in other studies (e.g., Hu & Wu, 2004; Ulbrich & Christoph, 1999) and associated with a change in midlatitude baroclinity and the intensity and position of the Atlantic jet stream and storm track. Previous studies (e.g., Stoner *et al*., 2009; Lee and Black, 2013; Davini and Cagnazzo, 2014; Ning and Bradley, 2016) also examine model biases in simulating and projecting the spatial NAO structure and link it to uncertainties related to internal model component variability or dynamics and emission scenarios.

Our simulations suggest an additional CSL decline of ca. 9 and 18 m by the end of the 21st century for the RCP4.5 and RCP8.5 scenarios, respectively, although this is only a first order estimate, neglecting any other water storage systems (e.g., groundwater) in the Caspian catchment basin, as well as discharge into the Kara-Bogaz bay, the CS bathymetry or tectonic movements (cf. Elguindi and Giorgi, 2006a; Elguindi and Giorgi, 2007). Moreover, these estimates must be taken with care since (a) no dynamic lake model is included in our simulations such that lake-climate feedbacks are not correctly captured, and (b) the Caspian lake area is too large in the CESM such that evaporation and hence the future CSL decrease are overestimated. The latter effect is of particular importance. Given that the present CS area and associated evaporation is about 10% less than in the model, a corrected CSL calculation with evaporation reduced by 10% yields CSL declines of ca. 8 and 16 m by the end of the 21st century for the RCP4.5 and RCP8.5 scenarios, respectively, still suggesting that evaporation plays a key role in future CSL evolution. Interestingly, a CSL rise in response to increasing greenhouse gas concentrations by the end of the 21st century was simulated with the coarse-resolution (2.5° horizontal grid resolution) ECHAM4 model (Arpe and Roeckner, 1999). However, this rise was estimated solely from the increase in the Volga river discharge due to increased winter circulation and precipitation. Other studies also find strongly increasing evaporation over the CS in response to increasing air temperatures and suggest CSL reductions by the end of the 21st century of at least 5 m in a regional model (Elguindi and Giorgi, 2007) and about 9 m in a multi-model (global) ensemble mean (Elguindi and Giorgi, 2006a). Taking all these estimates together, it appears highly likely that the CSL will substantially drop due to increased evaporation by the end of the century.

Indeed, Chen *et al*. (2017) recently suggested that increased evaporation over the Caspian Sea is not balanced by river discharge or precipitation, making it the leading driver for changes in CSL. This imbalance is likely to continue unless compensated by discharge or precipitation increases in the Caspian basin. However, that study did not provide specific estimates of the CSL changes by the end of the 21st century. If the current

rate of 7 cm/yr decrease in CSL (Chen *et al*., 2017) continues, the northern portion of the CS, in which water depths are less than 5 m, may disappear in 75 years. However, due to the strong interdecadal variability of the CSL, such a linear extrapolation should not be based on a decadal trend. Nevertheless, it cannot be ruled out that the shallow northern CS, like the nearby Aral Sea, could face similar catastrophic ecosystem and agricultural impacts (Kosarev, 2005). The middle and south Caspian basins are less likely to face such strong impacts due to greater depths of >800 m (Rodionov, 1994).

As mentioned above, a key caveat in this and other studies is related to the lack of feedbacks associated with a changing lake surface area. For example, a negative feedback where reduced Volga river discharge causes CSL lowering, lake surface area shrinking and hence decreasing evaporation is not modelled by CESM or other climate models. Arpe *et al*. (2019) suggest a formula to estimate this effect for correction. The correct size of the CS in climate models is important for simulating the hydrological cycle. Our simulations also do not consider human-made contributions to the CSL such as dam building and irrigation which may impact the hydrological cycle and the CS size. Further caveats include shortcomings in the simulation of orographic precipitation due to limited model resolution in particular in the Caucasus and Elburz mountain regions as well as the fact of not considering the effects of ENSO, which have been previously investigated in Arpe *et al*. (2000). Our study also highlights the need for evaluating and improving the atmospheric circulation patterns at mid-latitudes in climate models.

## 5 | CONCLUSIONS

Using the global climate model CESM1.2.2 we analysed the leading modes of North Atlantic winter climate variability and atmospheric teleconnection patterns in the Caspian catchment region for the past and future time interval 1850–2100. Our study reveals that CESM1.2.2 with CAM5 atmosphere physics and 1° resolution shows best skill in simulating the first mode when compared to the 1° CAM4 or 2° CAM4 setups. Under the RCP4.5 and RCP8.5 scenarios, the EOF-derived NAO remains the leading mode of winter North Atlantic climate variability, however the location and magnitudes of the centres of action change which affects the regional hydroclimate variability. An increased impact of the NAO on the Caspian region winter climate during the 21st century is seen for the RCP4.5 scenario with enhanced precipitation over the Volga basin during the positive NAO phase due to an intensified and easterly displaced northern centre of action. For RCP8.5 the effect of the NAO on P-E over the southern part of the CS catchment area increases such that a distinct P-E dipole emerges which results in a net cancellation of the NAO effect on the total Caspian water budget. Our results therefore suggest that the correlation between the NAO and the winter conditions over the CS catchment area depends on the changing background climate and on shifts in the location and magnitude of the NAO centres of action.

The most important effect of future warming on the CSL is related to increasing evaporation over the lake surface. Despite increasing precipitation over the northern Volga basin, the increasing evaporation results in a negative water budget and an additional CSL drop of ca. 9 m (RCP4.5) to 18 m (RCP8.5) in our CESM1.2.2 simulations by the end of the 21st century. Although these values may be somewhat overestimated due to a CS area that is too large in the model, our study still suggests a larger CSL drop than values presented in previous model studies. Such a CSL decline may have a significant impact on the Caspian environment especially over the northern Caspian basin which presently has a depth of less than 5 m. A logical next step is to study the robustness of our results by using multiple global and regional climate models.

## ACKNOWLEDGEMENTS

We thank two anonymous reviewers for their very helpful and constructive comments. This research was supported by the project PRIDE (Pontocaspian RIse and DEmise) which has received funding from the European Union's Horizon 2020 research and innovation program, under the Marie Sklodowska-Curie grant agreement No 642973. All CESM simulations were performed on the supercomputer of the Norddeutscher Verbund für Hoch- und Höchstleistungrechnen (HLRN-III). The authors declare no conflict of interests.

## ORCID

*Sri D. Nandini-Weiss* https://orcid.org/0000-0003-0869-0731

## REFERENCES

Aondover, T. (2013) *Climate Variability- Regional And Thematic Patterns*. London, England: IntechOpen Limited.

Arpe, K., Bengtsson, L., Golitsyn, S., Mokhov, I.I., Semenov, V.A. and Sporyshev, P.V. (1999) Analysis and modeling of the hydrological regime variations in the Caspian Sea basin. *Dokl., Earth Sci.*, 366(4), 552–556.

Arpe, K., Bengtsson, L., Golitsyn, S., Mokhov, I.I., Semenov, V.A. and Sporyshev, P.V. (2000) Connection between Caspian Sea level variability and ENSO. *Geophysical Research Letters*, 27, 2693–2696.

Arpe, K. and Leroy, S. (2007) The Caspian Sea level forced by the atmospheric circulation, as observed and modelled. *Quaternary International*, 173–174, 144–152.

Arpe, K., Leroy, S.A.G., Wetterhall, F., Khan, V., Hagemann, S. and Lahijani, H. (2014) Prediction ofthe Caspian Sea level using

ECMWF seasonal forecasts and reanalysis. *Theoretical and Applied Climatology*, 117(1–2), 41–60. https://doi.org/10.1007/s00704-013-0937-6

Arpe, K. and Roeckner, E. (1999) Simulation of the hydrologic cycle over Europe: model validation and impacts of increasing greenhouse gases. *Adv. Water Res*, 23, 105–119.

Arpe, K., Tsuang, B., Tseng, Y., Liu, X. and Leroy, S.A.G. (2019) Quantification of climatic feedbacks on the Caspian Sea level variability and impacts from the Caspian Sea on the large-scale atmospheric circulation. *Theoretical and Applied Climatology*. 136, 475–488. https://doi.org/10.1007/s00704-018-2481-x.

Barnston, A.G. and Livezey, R.E. (1987) Classifications, seasonality, and persistence of low-frequency atmospheric circulation patterns. *Monthly Weather Review*, 115, 1083–1126.

Baker, N.C. and Taylor, P.C. (2016) A framework for evaluating climate model performance metrics. *Journal of Climate*, 29, 1773–1782. https://doi.org/10.1175/JCLI-D-15-0114.1

Bueh, C. and Nakamura, H. (2007) Scandinavian pattern and its climatic impact. *Quarterly Journal of the Royal Meteorological Society*, 133, 2117–2131.

Chang, E.K.M., Guo, Y. and Xia, X. (2012) CMIP5 multimodel ensemble projection of storm track change under global warming. *Journal of Geophysical Research: Atmospheres*, 117(D23), 1–19. https://doi.org/10.1029/2012jd018578.

Chen, J.L., Pekker, T., Wilson, C.R., Tapley, B.D., Kostianoy, A.G., Cretaux, J.F. and Safarov, E.S. (2017) Long-term Caspian Sea level change. *Geophysical Research Letters*, 44, 6993–7001. https://doi.org/10.1002/2017GL073958.

Collins, M., Knutti, R., Arblaster, J., Dufresne, J.-L., Fichefet, T., Friedlingstein, P., et al. (2013) Long-term climate change: projections, commitments and irreversibility. In: Stocker, T.F., Qin, D., Plattner, G.-K., Tignor, M., Allen, S.K., Boschung, J., Nauels, A., Xia, Y., Bex, V. and Midgley, P.M. (Eds.) *Climate Change 2013: The Physical Science Basis. Contribution of Working Group I to the Fifth Assessment Report of the Intergovernmental Panel on Climate Change*. Cambridge, UK and New York, NY: Cambridge University Press, pp. 1029–1136.

Comas-Bru, L. and McDermott, F. (2014) Impacts of the EA and SCA patterns on the European twentieth century NAO–winter-climate relationships. *Quarterly Journal of the Royal Meteorological Society*, 140, 354–363. https://doi.org/10.1002/qj.2158.

Davini, P. and Cagnazzo, C. (2014) On the misinterpretation of the North Atlantic Oscillation in CMIP5 models. *Climate Dynamics*, 43(5), 1497–1511. https://doi.org/10.1007/s00382-013-1970-y.

Dee, D.P., Uppala, S.M., Simmons, A.J., Berrisford, P., Poli, P., Kobayashi, S., Andrae, U., Balmaseda, M.A., Balsamo, G., Bauer, P., Bechtold, P., Beljaars, A.C.M., van de Berg, L., Bidlot, J., Bormann, N., Delsol, C., Dragani, R., Fuentes, M., Geer, A.J., Haimberger, L., Healy, S.B., Hersbach, H., Hólm, E.V., Isaksen, L., Kållberg, P., Köhler, M., Matricardi, M., McNally, A. P., Monge-Sanz, B.M., Morcrette, J.J., Park, B.K., Peubey, C., de Rosnay, P., Tavolato, C., Thépaut, J.N. and Vitart, F. (2011) The ERA-interim reanalysis: configuration and performance of the data assimilation system. *Quarterly Journal of the Royal Meteorological Society*, 137(656), 553–597. https://doi.org/10.1002/qj.828.

Deser, C., Hurrell, J.W. and Phillips, A. (2017) The role of the North Atlantic Oscillation in European climate projections. *Climate Dynamics*, 49(9–10), 3141–3157.

Elguindi, N. and Giorgi, F. (2006a) Projected changes in the Caspian Sea level for the 21st century based on the latest AOGCM simulations. *Geophysical Research Letters*, 33(8), 1–4. https://doi.org/10.1029/2006GL025943.

Elguindi, N. and Giorgi, F. (2006b) Simulating multi-decadal variability of Caspian Sea level changes using regional climate model outputs. *Climate Dynamics*, 26, 167–181.

Elguindi, N. and Giorgi, F. (2007) Simulating future Caspian Sea level changes using regional climate model outputs. *Climate Dynamics*, 28, 365–379.

Gent, P.R., Danabasoglu, G., Donner, J.L., Holland, M.M., Hunke, E. C., Jayne, S.R., et al. (2011) The community climate system model version 4. *Journal of Climate*, 24(4973–4991), 4973–4991.

Golitsyn, G.S., Dzyuba, A.V., Osipov, A.G. and Panin, G.N. (1990) Regional climate changes and their manifestations in the present-day rise in the Caspian Sea level. *Doklady Akademii Nauk SSSR*, 313(5), 1224–1227.

Hunke, E. C., & Lipscomb, W. H. (2010). CICE: The Los Alamos Sea Ice Model, Documentation and Software User's Manual, Version 4.1. LA-CC-06-012, Los Alamos National Laboratory, N.M.

Hurrell, J.W. (1995) Decadal trends in the North-Atlantic Oscillation: regional temperatures and precipitation. *Science*, 269, 676–679.

Hurrell, J.W. and Deser, C. (2009) North Atlantic climate variability: the role of the North Atlantic Oscillation. *Journal of Marine Systems*, 78(1), 28–41. https://doi.org/10.1016/j.jmarsys.2008.11.026.

Hurrell, J.W., Holland, M.M. and Gent, P.R. (2013) The community earth system model: A framework for collaborative research. *Bulletin of the American Meteorological Society*, 94(9), 1339–1360.

Hurrell, J.W., Kushnir, Y., Ottersen, G. and Visbeck, M. (Eds.) (2003) The north atlantic oscillation: climate significance and environmental Impact. *Geophysical Monograph Series* (Vol. 134). Washington, DC: AGU.

Hurrell, J.W. and van Loon, H. (1997) Decadal variations in climate associated with the North Atlantic Oscillation. *Climatic Change*, 36 (3), 301–326. https://doi.org/10.1023/a:1005314315270.

Kalnay, E., Kanamitsu, M., Kistler, R., Collins, W., Deaven, D., Gandin, L., Iredell, M., Saha, S., White, G., Woollen, J., Zhu, Y., Leetmaa, A., Reynolds, R., Chelliah, M., Ebisuzaki, W., Higgins, W., Janowiak, J., Mo, K.C., Ropelewski, C., Wang, J., Jenne, R. and Joseph, D. (1996) The NCEP/NCAR 40-year reanalysis project. *Bulletin of the American Meteorological Society*, 77, 437–471.

Kislov, A.V., Panin, A. and Toropov, P.A. (2014) Current status and palaeostages of the Caspian Sea as a potential evaluation tool for climate model simulations. *Quaternary International*, 345, 48–55. https://doi.org/10.1016/j.quaint.2014.05.014.

Kislov, A.V. and Toropov, P.A. (2007) Climate modeling results for the circum-Pontic region from the late Pleistocene to the mid-Holocene. In: Yanko-Hombach, V., Gilbert, A.S., Panin, N. and Dolukhanov, P.M. (Eds.) *Book on "The Black Sea Flood Question: Changes in Coastline, Climate, and Human Settlement"*. Dordrecht: Springer, pp. 47–62.

Kosarev, A.N. (2005) Physico-geographical conditions of the Caspian Sea. In: Kostianoy, A.G. and Kosarev, A.N. (Eds.) *The Caspian Sea Environment*. Berlin and Heidelberg, Germany: Springer.

Kroonenberg, S.B., Kasimov, N.S. and Lychagin, M.Y. (2008) The Caspian Sea: A natural laboratory for sea-level change. *Geography, Environment, Sustainability*, 1, 22–37.

Lamarque, J.-F., Kyle, G.P., Meinshausen, M., Riahi, K., Smith, S.J., van Vuuren, D.P., Conley, A.J. and Vitt, F. (2011) Global and regional evolution of short-lived radiatively-active gases and aerosols in the representative concentration pathways. *Climatic Change*, 109(1), 191–212. https://doi.org/10.1007/s10584-011-0155-0.

Lawrence, D.M., Oleson, K.W., Flanner, M.G., Thornton, P.E., Swenson, S.C., Lawrence, P.J., Zeng, X., Yang, Z.L., Levis, S., Sakaguchi, K., Bonan, G.B. and Slater, A.G. (2011) Parameterization improvements and functional and structural advances in version 4 of the community land model. *Journal of Advances in Modeling Earth Systems*, 3(1), 1–27. https://doi.org/10.1029/2011ms00045.

Lee, Y.-Y. and Black, R.X. (2013) Boreal winter low-frequency variability in CMIP5 models. *Journal of Geophysical Research: Atmospheres*, 118(13), 6891–6904. https://doi.org/10.1002/jgrd.50493.

Leroy, S. A. G., Lahijani, H., Crétaux, J.-F., Aladin, N., & Plotnikov, I. (accepted 2019). Past and current changes in the largest lake of the world: The Caspian Sea. In M. S. (Ed.), *Large Asian Lakes in a Changing World*. New York, NY: Springer.

Meehl, G., Stocker, T., Collins, W. D., Friedlingstein, P., Gaye, A. T., Gregory, J. M., et al. (2007). *Global climate projections climate change* 2007*: The physical science basis*.

Meehl, G.A., Washington, W.M., Arblaster, J.M., Hu, A., Teng, H., Tebaldi, C., Sanderson, B.N., Lamarque, J.F., Conley, A., Strand, W.G. and White, J.B., III. (2012) Climate system response to external Forcings and climate change projections in CCSM4. *Journal of Climate*, 25(11), 3661–3683. https://doi.org/10.1175/jcli-d-11-00240.1.

Meinshausen, M., Smith, S.J., Calvin, K.V., Daniel, J.S., Kainuma, M.L. T., Lamarque, J.F., et al. (2011) The RCP greenhouse gas concentrations and their extension from 1765 to 2300. *Climatic Change*, 109 (Special Issue), 213. https://doi.org/10.1007/s10584-011-0156-z.

Molavi-Arabshahi, M., Arpe, K. and Leroy, S. (2015) Precipitation and temperature of the Southwest Caspian Sea region during the last 55 years: their trends and teleconnections with large-scale atmospheric phenomena. *International Journal of Climatology*, 36, 2156–2172.

Moss, R. H., Edmonds, J. A., Hibbard K. A., Manning M. R., Rose S. K., van Vuuren D. P., et al. (2010). The next generation of scenarios for climate change research and assessment. *Nature Climate Change*, 463, 747–756.

Neale, R. B., Gettelman, A., Park, S., Chen, C. C., Lauritzen, P. H., Williamson, D. L., et al. (2012). *Description of the NCAR Community Atmosphere Model (CAM 5.0)*. Retrieved from Boulder, Colorado, USA

Ning, L. and Bradley, R.S. (2016) NAO and PNA influences on winter temperature and precipitation over the eastern United States in CMIP5 GCMs. *Climate Dynamics*, 46(3), 1257–1276. https://doi.org/10.1007/s00382-015-2643-9.

North, G.R., Bell, T.L., Cahalan, R.F. and Moeng, F.J. (1982) Sampling errors in the estimation of empirical orthogonal functions. *Monthly Weather Review*, 110(7), 699–706. https://doi.org/10.1175/1520-0493.

Panin, G.N. and Dianskii, N.A. (2014) On the correlations between oscillations of the Caspian Sea level and North Atlantic climate. *Izvestiya, Atmospheric & Oceanic Physics.*, 50(3), 266–277. https://doi.org/10.1134/S000143381402008X.

Panin, G.N., Solomonova, I.V. and Vyruchalkina, T.Y. (2014) Regime of water balance components of the Caspian Sea. *Water Resources*, 41(5), 505–511.

Panin, G.N., Vyruchalkina, T.Y. and Solomonova, I.V. (2015) Effect of the North Atlantic on the hydrological regime of the Caspian Sea Basin. *Water Resources*, 42(4), 525–534.

Renssen, H., Longhead, B.C., Aerts, J.C., de Moel, H., Ward, P.J. and Kwadijk, J.C.J. (2007) Simulating long-term Caspian Sea level changes; the impact of Holocene and future climate conditions. *Earth and Planetary Science Letters*, 261, 685–693.

Rodionov, S. (1994) *Global and Regional Climate Interaction: The Caspian Sea Experience*. New York, NY: Springer.

Smith, R., Jones, P., Briegleb, B., Bryan, F., Danabasoglu, G., Dennis, J., et al. (2010). The parallel ocean program (POP) reference manual: Ocean component of the community climate system model (CCSM). *Tech. Note LAUR-10-01853, Los Alamos Natl.* Lab., Los Alamos, N. M.

Stoner, A.M.K., Hayhoe, K. and Wuebbles, D.J. (2009) Assessing general circulation model simulations of atmospheric Teleconnection patterns. *Journal of Climate*, 22(16), 4348–4372. https://doi.org/10.1175/2009jcli2577.1.

Taylor, K.E. (2001) Summarizing multiple aspects of model performance in a single diagram. *JGR*, 106, 7183–7192.

Trigo, R.M., Osborn, T.J. and Corte-Real, J.M. (2002) The North Atlantic oscillation influence on Europe climate impacts and associated physical mechanisms. *Climate Research*, 20(1), 9–17.

van Vuuren, D.P., Edmonds, J., Kainuma, M., Riahi, K., Thomson, A., Hibbard, K., Hurtt, G.C., Kram, T., Krey, V., Lamarque, J.F., Masui, T., Meinshausen, M., Nakicenovic, N., Smith, S.J. and Rose, S.K. (2011) The representative concentration pathways: an overview. *Climatic Change*, 109(1), 5–31. https://doi.org/10.1007/s10584-011-0148-z.

Ulbrich, U. and Christoph M. (1999) A shift of the NAO and increasing storm track activity over Europe due to anthropogenic greenhouse gas forcing. *Climate Dynamics*, 15, 551–559.

Wang, W., Lee, X., Xiao, W., Liu, S., Schultz, N., Wang, Y., Zhang, M. and Zhao, L. (2018) Global lake evaporation accelerated by changes in surface energy allocation in a warmer climate. *Nature Geoscience*, 11(6), 410–414. https://doi.org/10.1038/s41561-018-0114-8.

Willmott, C.J. and Matsuura, K. (1995) Smart interpolation of annually averaged air temperature in the United States. *Journal of Applied Meteorology*, 34, 2577–2586.

Yanina, T.A. (2014) The Ponto-Caspian region: environmental consequences of climate change during the late Pleistocene. *Quaternary International*, 345, 88–99. https://doi.org/10.1016/j.quaint.2014.01.045.

Yin, J.H. (2005) A consistent poleward shift of the storm tracks in simulations of 21st century climate. *Geophysical Research Letters*, 32 (18), 1–4. https://doi.org/10.1029/2005gl023684.

Zeng-Zhen, H. and Zhaohua, W. (2004) The intensification and shift of the annual North Atlantic Oscillation in a global warming scenario simulation. *Tellus A: Dynamic Meteorology and Oceanography*, 56 (2), 112–124. https://doi.org/10.3402/tellusa.v56i2.14403.

## SUPPORTING INFORMATION

Additional supporting information may be found online in the Supporting Information section at the end of this article.

**How to cite this article:** Nandini-Weiss SD, Prange M, Arpe K, Merkel U, Schulz M. Past and future impact of the winter North Atlantic Oscillation in the Caspian Sea catchment area. *Int J Climatol*. 2020;40:2717–2731. https://doi.org/10.1002/joc.6362